On the Statistical Performance of Connectivity Estimators in the Frequency Domain

Koichi Sameshima[1], Daniel Y. Takahashi[2], and Luiz A. Baccalá[3]

[1] Department of Radiology and Oncology, Faculdade de Medicina,
University of São Paulo, São Paulo, SP, 01246-903, Brazil
ksameshi@usp.br
[2] Psychology Department, Neuroscience Institute,
Princeton University, Princeton, NJ, USA
[3] Department of Telecommunications and Control Engineering, Escola Politécnica,
University of São Paulo, São Paulo, SP, Brazil

Abstract. This paper studies the performance of recently introduced asymptotic statistics for connectivity inference in the frequency domain, namely via information partial directed coherence (iPDC) and information directed transfer function (iDTF) and compares them to the behaviour of a classic time domain multivariate Granger causality test (GCT) by using Monte Carlo simulations of three widely used toy-models under varying the simulated data record lengths. In general, the false-positive rates for non-existing connections and the false-negative rates for existing connections are found to decrease with longer record lengths.

Keywords: Partial Directed Coherence, Directed Transfer Function, Granger Causality, Null hypothesis test performance.

1 Introduction

This paper examines the comparative statistical performance of the connectivity detection problem [1] for three popular neural connectivity estimators that enjoy rigorously known description of their asymptotic behaviour. In addition to the Granger causality test (GCT) from [2], we recently derived rigorous results [3,4] about the asymptotic behaviour of information partial directed coherence (iPDC) and information directed transfer function (iDTF) [5] which are quantities that respectively generalize *partial directed coherence* (PDC) [6] and *directed transfer function* (DTF) [7] to correctly describe coupling size effect issues.

Exploiting three widely used toy models selected from the literature, we carried out Monte Carlo simulations to verify the performance of the connectivity null hypothesis under their derived optimum rejection criteria as a function of data record length (K) showing them compatible with their expected large sample behaviour. We complemented the study by computing false-positive and false-negative test rates for each estimator alternative.

D. Ślęzak et al. (Eds.): BIH 2014, LNAI 8609, pp. 412–423, 2014.

2 Methods and Results

2.1 Monte Carlo Simulations

Following our recently proposed the information PDC and information DTF [5], and their corresponding rigorous asymptotic statistics for both measures (see [3] and [4] for details) we here examine their statistical performance against that of the well-established time-domain GCT [2]. We do so via Monte Carlo simulations performed in the MATLAB environment by using its "normally distributed pseudorandom number" generator to simulate system innovation noise processes, which were furthermore assumed zero mean unit variance and uncorrelated. To test the performance of the latter three connectivity estimators, for each toy model and at each data record length we selected $K = \{100, 200, 500, 1\,000, 2\,000, 5\,000, 10\,000\}$ repeating 1 000 simulations for each case. For each simulation, the first 5 000 data points were discarded to eliminate possible transients. We used the Nuttal-Strand algorithm for multivariate autoregressive (MAR) model estimation and the Akaike information criterion (AIC) for model order selection [8]. *i*PDC and *i*DTF detection threshold was set for $\alpha = 1\%$ and p-values were computed at in 32 uniformly separated normalized frequency points covering the whole interval.

A connection was deemed detected for a given pair of structures if its p-value resulted less than α for some frequency within the interval. This connectivity decision criterion is somewhat lax and tends to overestimate the presence connectivity for *i*PDC and *i*DTF. In particular for *i*PDC, it should detect connectivity more often than GCT does.

The reader may access our open MATLAB codes for both *i*PDC and *i*DTF asymptotic statistics used in this study at www.lcs.poli.usp.br/∼baccala/pdc.

Next we describe and probe the toy models:

2.2 Model 1: Closed-Loop Model

Model 1 is an $\{N = 7\}$-variable model borrowed from [9] (Fig. 1). It has two distinct disconnected substructures: $\{x_1, x_2, x_3, x_4, x_5\}$ and $\{x_6, x_7\}$, which share a same common frequency of oscillation. The set of equations that describes the model is:

$$\begin{cases} x_1(t) = 0.95\sqrt{2}x_1(t-1) - 0.9025x_1(t-2) + 0.5x_5(t-2) + w_1(t) \\ x_2(t) = -0.5x_1(t-1) + w_2(t) \\ x_3(t) = 0.4x_2(t-2) + w_3(t) \\ x_4(t) = -0.5x_3(t-1) + 0.25\sqrt{2}x_4(t-1) + 0.25\sqrt{2}x_5(t-1) + w_4(t) \\ x_5(t) = -0.25\sqrt{2}x_4(t-1) + 0.25\sqrt{2}x_5(t-1) + w_5(t) \\ x_6(t) = 0.95\sqrt{2}x_6(t-1) - 0.9025x_6(t-2) + w_6(t) \\ x_7(t) = -0.1x_6(t-1) + w_7(t) \end{cases} \quad (1)$$

with w_i standing for innovation noises.

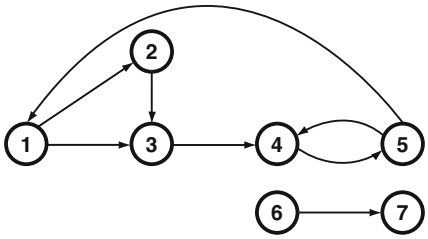

Fig. 1. Diagram depicting the essential elements of Model 1 represented by Eq. 1 from [9]. The elements x_1 to x_5 establish closed-loop connections, with short and long connected paths, while x_6 and x_7 are part of completely separate substructure, i.e. disconnected from $\{x_1, ..,x_5\}$, but sharing a common frequency of oscillation.

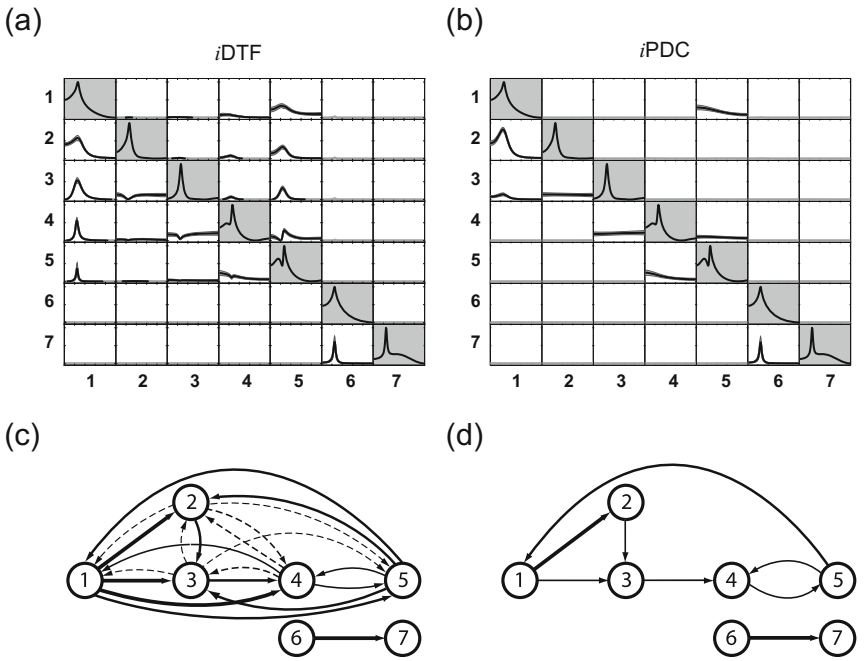

Fig. 2. This figure depicts the result of (**a**) iDTF and (**b**) iPDC estimations obtained with a data simulation of Model 1, given by Eq. 1, with $K = 2\,000$ points and $\alpha = 1\%$, where standard subplotting lay-out with variables in columns representing the source and in rows the target structures is used, and in each subplot the x-axis represents the frequency and y-axis the iDTF and iPDC scaled in [0 1] interval. The main-diagonals with grayed-background subplottings contain the power spectra. (**c**) Note, as theoretically expected, that according to iDTF estimation nodes can reach one another among $\{x_1, x_2, x_3, x_4, x_5\}$, as although some magnitudes of iDTF are very small, they are all statistically significant. (**d**) While iPDC estimate shows immediate adjacent node connectivity pattern.

A single trial example of iDTF and iPDC connectivity estimation in the frequency domain are respectively depicted in Figs. 2 **a** and **b**, with significant values, at $\alpha = 0.01$, represented by black solid lines. The corresponding connectivity graph diagrams are contained in Figs. 2 **c** and **d**, where arrow thickness represents estimate magnitude. Note that iPDC reflects adjacent connections Fig. 2**b** and **d**, while iDTF represents reachability aspects of the directed structure [10].

Granger Causality Test for Model 1. Fig. 3 summarizes the performance of Granger causality test for data record lengths $K = \{100, 200, 500, 1\,000, 2\,000, 5\,000\}$. As expected, for $K > 200$, GCT properly detects the connectivity presence and absence.

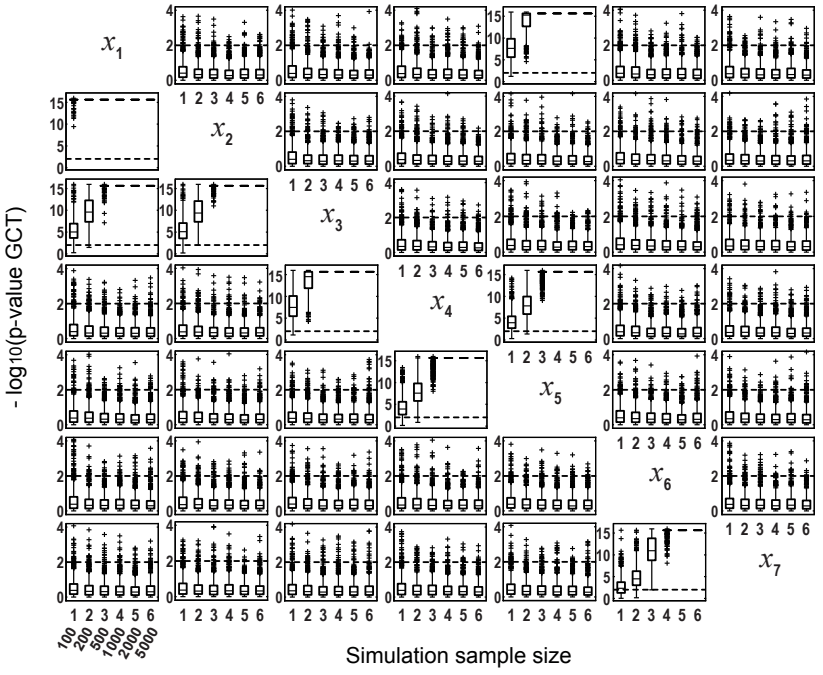

Fig. 3. In this and all the figures that follow, the pattern contains subplots with variables in columns representing the sources and while the target structures lie in rows. Each subplot possesses boxplots of the distribution of $-log_{10}(p\text{-value})$ for Granger causality test for 1 000 Monte Carlo simulations over different record lengths $K = \{100, 200, 500, 1\,000, 2\,000, 5\,000\}$, marked as 1, 2, 3, 4, 5 and 6, respectively, on the x-axis of each subplot. Since $\alpha = 0.01$ values above 2 (dashed-line) indicate rejection of the null-hypothesis of connectivity absence.

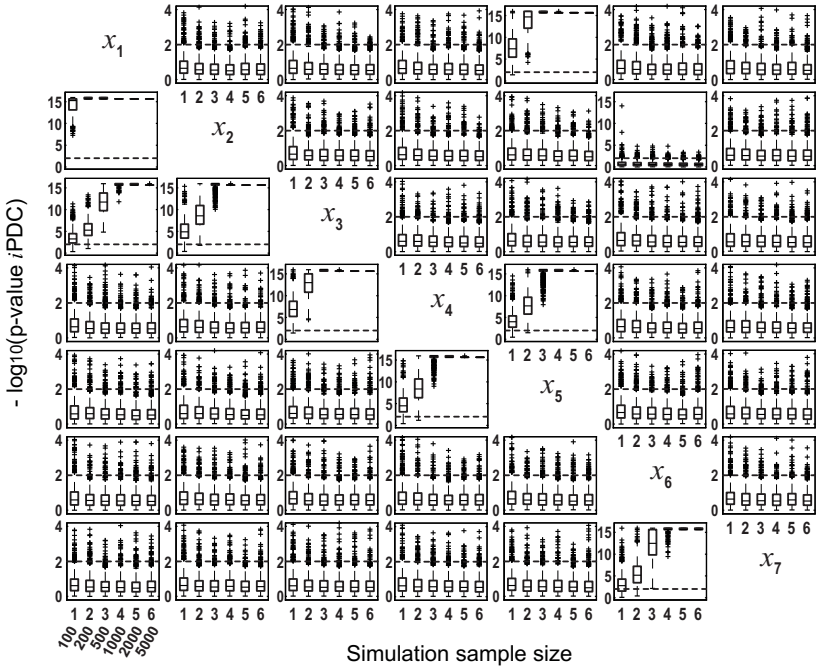

Fig. 4. Model 1 boxplot performance summary of iPDC asymptotics

Information Partial Directed Coherence Asymptotics Performance for Model 1. Fig. 4 summarizes the performance of asymptotic statistics for iPDC for the Model 1 for the same data and record lengths as those for GCT. As can be seen comparing Figs. 3 and 4, iPDC's asymptotic performance is similar to GCT's.

Information Directed Transfer Function Asymptotics Performance for Model 1. Fig. 5 summarizes the performance of the asymptotic statistics for iDTF. The boxplots clearly show that for larger sample size iDTF correctly detects the reachability structure shown in Fig. 2**c**. Note that the weakest or farthest connection ($x_2 \to x_1$) requires longer record lengths for proper detection. A modified DTF measure combined with partial coherence, called direct directed transfer function (dDTF) [11], was not explored here as its asymptotic statistics are not yet available.

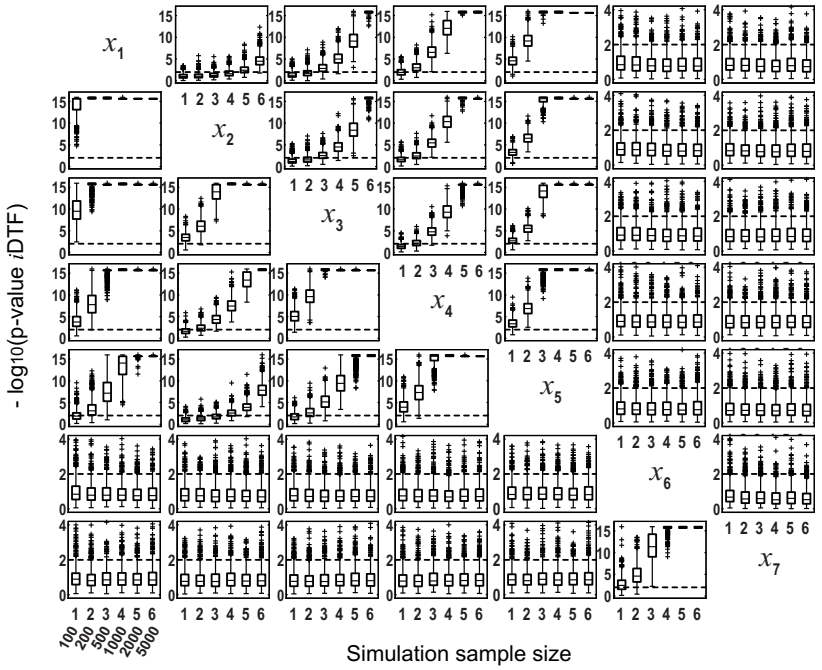

Fig. 5. Model 1 boxplot performance summary of iDTF asymptotics

2.3 Model 2: Five-Variable Model

Model 2 is graphically represented in Fig. 6 with its corresponding set of defining equations:

$$\begin{cases} x_1(t) = 0.95\sqrt{2}x_1(t-1) - 0.9025x_1(t-2) + w_1(t) \\ x_2(t) = 0.5x_1(t-2) + w_2(t) \\ x_3(t) = -0.4x_1(t-3) + w_3(t) \\ x_4(t) = -0.5x_1(t-2) + 0.25\sqrt{2}x_4(t-1) + 0.25\sqrt{2}x_5(t-1) + w_4(t) \\ x_5(t) = -0.25\sqrt{2}x_4(t-1) + 0.25\sqrt{2}x_5(t-1) + w_5(t) \end{cases} \tag{2}$$

where w_i stand for unit variance uncorrelated zero mean Gaussian innovations.

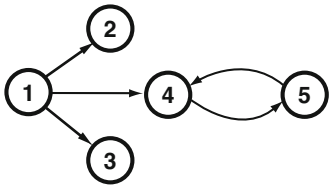

Fig. 6. Diagram depicting the essential elements of Model 2 introduced by [6]

Granger Causality Test Performance. Using $K = \{100, 200, 500, 1\,000, 2\,000\}$ for Model 2, Fig. 7 shows that GCT's performance improves with increased record length. At $K = 200$, GCT already performs well with false-negative rate bellow 5%, reaching false-negative rates below 2% for $K = 2\,000$.

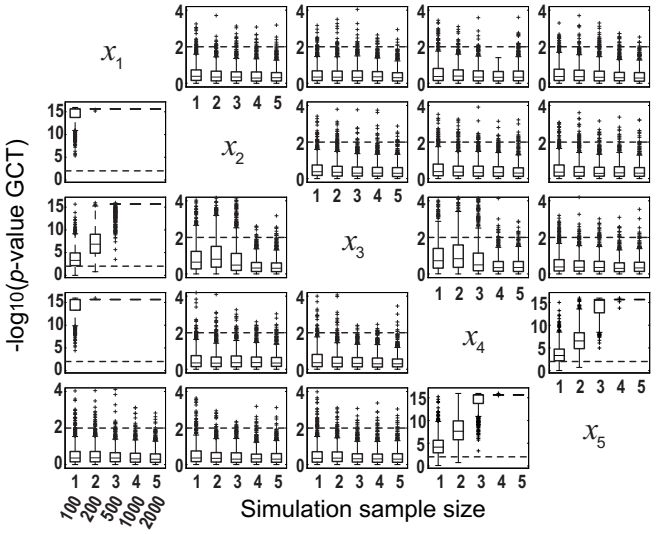

Fig. 7. GCT performance for Model 2

***i*PDC Asymptotics Performance for Model 2.** For Model 2, as seen in Fig. 8, the pattern of *i*PDC performance is similar to GCT's. Yet *i*PDC's false-negative rates are slightly higher than GCT's. For example its performance for $K = 2\,000$ is between 3.0% and 5.5%. False-negative rates are practically negligible when $K > 200$ for both GCT and *i*PDC.

2.4 Model 3: Modified Five-var Model

To further probe the statistical behaviour of GCT and *i*PDC, we simulated the five-channel toy model originally introduced in [6] under a variant of its formulation as proposed by [12] reproduced here for reference in Fig. 9.

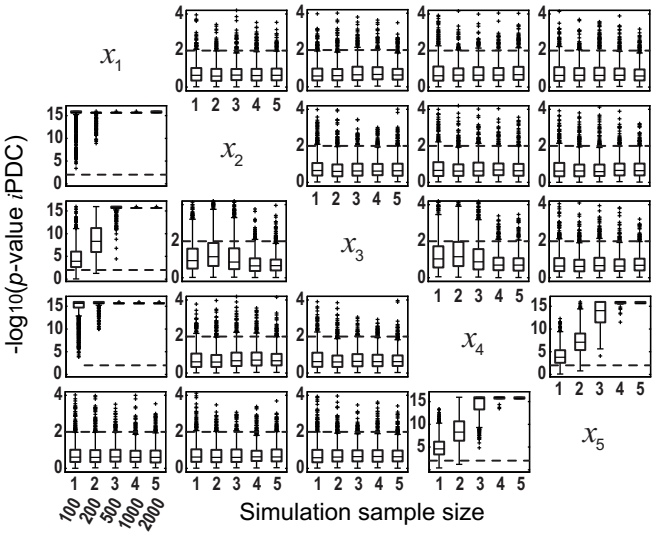

Fig. 8. *i*PDC performance for Model 2

The corresponding set of equations is given by

$$\begin{cases} x_1(t) = 0.95\sqrt{2}x_1(t-1) - 0.9025x_1(t-2) \\ \qquad + e_1(t) + a_1e_6(t) + b_1e_7(t-1) + c_1e_7(t-2) \\ x_2(t) = 0.5x_1(t-2) \\ \qquad + e_2(t) + a_2e_6(t) + b_2e_7(t-1) + c_2e_7(t-2) \\ x_3(t) = -0.4x_1(t-3) \\ \qquad + e_3(t) + a_3e_6(t) + b_3e_7(t-1) + c_3e_7(t-2) \\ x_4(t) = -0.5x_1(t-2) + 0.25\sqrt{2}x_4(t-1) + 0.25\sqrt{2}x_5(t-1) \\ \qquad + e_4(t) + a_4e_6(t) + b_4e_7(t-1) + c_4e_7(t-2) \\ x_5(t) = -0.25\sqrt{2}x_4(t-1) + 0.25\sqrt{2}x_5(t-1) \\ \qquad + e_5(t) + a_5e_6(t) + b_5e_7(t-1) + c_5e_7(t-2) \end{cases} \tag{3}$$

additionally containing the large exogenous input $e_6(t)$ and the latent variable $e_7(t)$. In the simulations $e_i(t)$ were uncorrelated zero mean unit variance Gaussian innovation noises and the parameters were chosen $a_i \sim U(0,1)$, $b_i = 2$ and $c_i = 5$, $i = 1, \ldots, 5$ as in [12]. Also for reference, $n_s = 2\,000$ data length were used in [12].

The proposal in [12] of introducing exogenous/latent variables is an interesting idea which allows investigating the influence of large common additive noise

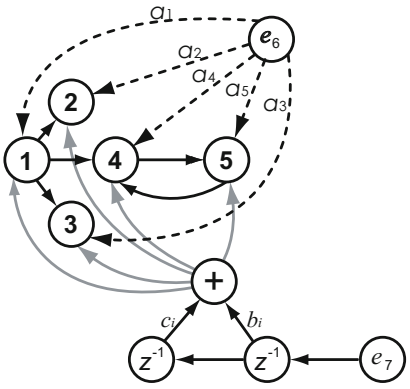

Fig. 9. Diagram depicting the essential elements of model introduced by [12] modified from [6]. For each simulation, the parameters a_i were chosen randomly from uniformly distributed [0 1] interval, and all $b_i = 2$ and $c_i = 5$, while the innovations, e_i, were drawn from random variables with $N\{0, 1\}$

sources on the performance of GCT and *i*PDC. Here, in order to assess the impairment that the extra exogenous/latent variables possibly inflict on null hypothesis testing, we repeated the procedure not just under the same conditions of [12], but also using a broader range of data record sizes:

$$K = \{100, 200, 500, 1\,000, 2\,000, 5\,000, 10\,000\}.$$

GCT Performance in the Presence of Exogenous Noise, Model 3. The GCT performance for Model 3 can be appreciated in Fig. 10. When compared with Model 2, GCT's performance deteriorates in the presence of exogenous noise. Interestingly its performance with respect to detecting existing connections increases with longer data records, while in absence of connections, the false-positive rate increases sharply for the $K = 10\,000$ case. For $K = 500$ the false-positive rates are around 5%, and increase to almost 40% for $K = 10\,000$. False-negative rates are negligible.

***i*PDC Performance in the Presence of Exogenous Noise.** As seen in Fig. 11, *i*PDC performance in detecting connectivity is similar to GCT's. As noted before, *i*PDC tends to have higher false-positive rates compared to GCT due to possibly the chosen frequency domain detection criterion of using a single-frequency with significant p-value as indicative of a valid connection.

The false-positive rates go from 10% for $K = 100$ up to 48% for $K = 10\,000$.

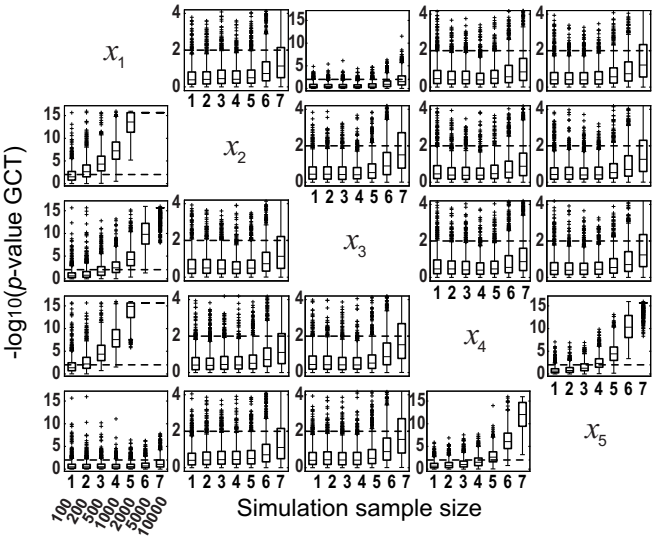

Fig. 10. GCT performance on Model 3

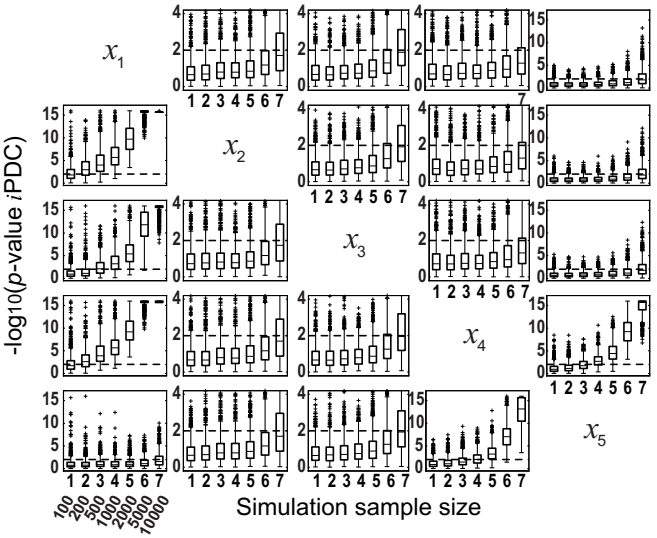

Fig. 11. *i*PDC performance on Model 3

3 Discussion

In this study we gathered simulation evidence of the performance of three statistical connectivity tests: one in time domain, usually considered as the gold-standard and two new frequency domain measures. The results are mutually corroborative.

The asymptotic results gauged via Monte Carlo simulations showed good large sample fit and robustness. In the presence of large exogenous/latent variables, we observed poor performance for large samples possibly due to the poor performance of MAR model estimation algorithm under low signal-to-noise ratio. Interestingly, however, a good performance was attained around $K = 2\,000$, as used by [12], for both GCT and *i*PDC (see Figs. 10 and 11). Current investigation is centered on comparing different algorithms for multivariate autoregressive estimation..

Acknowledgements. CNPq Grants 307163/2013-0 to L.A.B. and 309381/2012-6 to K.S. are also gratefully acknowledged and to NAPNA - Núcleo de Neurociência Aplicada from the University of São Paulo. Part of this work took place during FAPESP Grant 2005/56464-9 (CInAPCe).

References

1. Baccalá, L.A., Sameshima, K.: Brain Connectivity: An Overview. In: Methods in Brain Connectivity Inference through Multivariate Time Series Analysis, pp. 1–9. CRC Press (2014)
2. Lütkepohl, H.: New Introduction to Multiple Time Series Analysis. Springer, New York (2005)
3. Baccalá, L., De Brito, C., Takahashi, D., Sameshima, K.: Unified asymptotic theory for all partial directed coherence forms. Philosophical Transactions of the Royal Society A: Mathematical, Physical and Engineering Sciences 371, 1–13 (2013)
4. Baccalá, L.A., Takahashi, D.Y., Sameshima, K.: Consolidating a link centered neural connectivity framework with directed transfer function asymptotic. Biological Cybernetics (submitted, 2014)
5. Takahashi, D., Baccalá, L., Sameshima, K.: Information theoretic interpretation of frequency domain connectivity measures. Biological Cybernetics 103, 463–469 (2010)
6. Baccalá, L.A., Sameshima, K.: Partial directed coherence: a new concept in neural structure determination. Biological Cybernetics 84, 463–474 (2001)
7. Kamiński, M., Blinowska, K.J.: A new method of the description of the information flow in brain structures. Biological Cybernetics 65, 203–210 (1991)
8. Marple Jr., S.: Digital Spectral Analysis. Prentice Hall, Englewood Cliffs (1987)
9. Baccalá, L.A., Sameshima, K.: Overcoming the limitations of correlation analysis for many simultaneously processed neural structures. Progress in Brain Research, Advances in Neural Population Coding 130, 33–47 (2001)

10. Baccalá, L.A., Sameshima, K.: Multivariate Time Series Brain Connectivity: A Sum Up. In: Methods in Brain Connectivity Inference through Multivariate Time Series Analysis, pp. 245–251. CRC Press, Boca Raton (2014)
11. Korzeniewska, A., Mańczak, M., Kamiński, M., Blinowska, K.J., Kasicki, S.: Determination of information flow direction among brain structures by a modified directed transfer function (dDTF) method. Journal of Neuroscience Methods 125, 195–207 (2003)
12. Guo, S., Wu, J., Ding, M., Feng, J.: Uncovering interactions in the frequency domain. PLoS Computational Biology 4, e1000087 (2008)